01 Jan 1967

Dynamic Response Of Plates Due To Moving Loads

Theodore F. Raske
Missouri University of Science and Technology

Alois L. Schlack

Recommended Citation

T. F. Raske and A. L. Schlack, "Dynamic Response Of Plates Due To Moving Loads," *Journal of the Acoustical Society of America*, vol. 42, no. 3, pp. 625 - 635, Acoustical Society of America, Jan 1967.
The definitive version is available at https://doi.org/10.1121/1.1910634

JULY 21 2005

Dynamic Response of Plates Due to Moving Loads

Theodore F. Raske; Alois L. Schlack, Jr.

J Acoust Soc Am 42, 625–635 (1967)
https://doi.org/10.1121/1.1910634

Received 15 August 1966

Dynamic Response of Plates Due to Moving Loads

THEODORE F. RASKE

Department of Engineering Mechanics, University of Missouri, Rolla, Missouri 65401

ALOIS L. SCHLACK, JR.

Department of Engineering Mechanics, University of Wisconsin, Madison, Wisconsin 53700

An analysis based on linear theory is presented for determining the dynamic response and the conditions of resonance for a simply supported rectangular plate acted upon by two types of moving loads corresponding to: (1) a point force of variable magnitude oscillating about a fixed position on the plate, and (2) a point force of constant magnitude traveling in a circular orbit about a fixed position on the plate. In addition to the ordinary resonance as produced by a variable magnitude load concentrated at a fixed position on the plate, resonance of the plate may occur due to the changing position of the load on the plate. It is shown that an infinitely countable number of load movement frequencies may excite a given principal frequency of the plate for the m, nth mode of vibration. Numerical examples of typical deflection profiles and time rate of deflection buildup are presented for two sets of initial conditions corresponding to: (1) a load initially at rest on the deflected beam, and (2) an accelerating load dropped from zero height on an initally undeformed beam.

LIST OF SYMBOLS

General

J_0	Bessel function or order zero	t	time
J_ν	Bessel function of integer order ν	X	amplitude of longitudinal oscillation of load
k	effective spring constant of elastic foundation	β	frequency of longitudinal oscillation of load
		ω	transverse frequency of load
P	magnitude of point load	δ	Dirac-delta symbol

Plate Symbols

a	length of plate	$w(x,y,t)$	deflection of plate
b	width of plate	ρ	mass per unit area of plate
D	flexural rigidity	τ	$(\pi^2/a^2)(D/\rho)^{\frac{1}{2}}t$
A_m	$m\pi x_0/a$		
A_n	$n\pi y_0/b$	$\bar{\beta}$	$\dfrac{\beta}{(\pi^2/a^2)(D/\rho)^{\frac{1}{2}}}$
B_m	$m\pi X/a$		
L	$4Pa^3/bD\pi^4$		
N_a, N_b	axial forces per unit length	$\bar{\omega}$	$\dfrac{\omega}{(\pi^2/a^2)(D/\rho)^{\frac{1}{2}}}$
R	radius of circular orbit		
R_m	$m\pi R/a$		
R_n	$n\pi R/b$	α_1	a/b
(x_0, y_0)	position on plate measured from coordinate axis	α_2	$(Na/D)(a^2/\pi^2)$
		α_3	$(Nb/D)(b^2/\pi^2)$

α_4 $(ka^4)/D\pi^4$
$W(x,y,\tau)$ $w(x,y,t)bD\pi^4/2Pa^3$
$\bar{\lambda}^2$ $[m^2+(\alpha_1 n)^2]^2+\alpha_2 m^2+\alpha_3(\alpha_1 n)^2+\alpha_4$

$$\nabla^4 \quad \frac{\partial^4}{\partial x^4}+2\frac{\partial^4}{\partial x^2\partial y^2}+\frac{\partial^4}{\partial y^4}$$

INTRODUCTION

THE dynamic response of elastic bodies to moving loads has been the subject of many investigations, and, consequently, an extensive bibliography is available. However, with few exceptions, these studies have been restricted to loads moving with uniform velocity. Solutions for a rectangular plate acted upon by uniformly moving loads have been presented by Nowacki,[1] Holl,[2] and Piszczek,[3] among others, where it was shown that a critcal velocity existed for each vibrational mode. Steady-state solutions for an infinite plate carrying a uniformly moving load were given by Reismann,[4] Livesley,[5] and Morley.[6]

This paper presents an analysis of the dynamic response of a simply supported rectangular plate acted upon by two types of moving loads corresponding to: (1) a point force of variable magnitude oscillating about a fixed position on the plate, and (2) a point force of constant magnitude traveling in a circular orbit about a fixed position on the plate. In addition to the ordinary resonace as produced by a variable-magnitude load concentrated at a fixed position on the plate, resonance of the plate may occur owing to the changing position of the load on the plate. It is shown that an infinitely countable number of load movement frequencies may excite a given principal frequency of the plate for the m, nth mode of vibration. Loadings of this type may occur on an elastic system by an externally forced motion of a loading mechanism, or as the result of longitudinal vibration of the load or supporting structure relative to one another.

I. ANALYSIS

The simply supported plate shown in Fig. 1 is loaded transversely by a moving time-dependent point force $P(t)$ whose instantaneous position on the plate is given by $x=x(t)$ and $y=y(t)$. In addition to simple supports at the edge of the plate, the plate may also be: (1) supported by an elastic foundation, which produces a restoring force on the plate proportional to its local deflection, and (2) loaded by constant axial forces N_a and N_b, which are not large enough to cause static buckling. The governing differential equation for the deflection of a thin, isotropic and homogeneous plate of constant thickness is

$$D\nabla^4 w+\rho\frac{\partial^2 w}{\partial t^2}-N_a\frac{\partial^2 w}{\partial x^2}-N_b\frac{\partial^2 w}{\partial y^2}+kw = P(t)\delta[x-x(t)]\cdot\delta[y-y(t)], \quad (1)$$

where $\delta(t)$ is the Dirac-delta function and $w=w(x,y,t)$.

Equation 1 is subject to the limitations imposed by the classical plate theory and is valid provided that the deflection of the median plane is small as compared to the plate thickness. In addition, the effects of transverse shear, rotary inertia, and damping have been neglected.

The solution of Eq. 1 for the case of a simply supported plate is sought in the form of the series

$$w(x,y,t)=\sum_{m=1}^{\infty}\sum_{n=1}^{\infty} w_{m,n}(t)\sin\frac{m\pi x}{a}\sin\frac{n\pi y}{b}, \quad (2)$$

where $w_{m,n}(t)$ are unknown functions of time. Substituting Eq. 2 into Eq. 1 and applying standard Fourier techniques, the following differential equation is obtained for each $w_{m,n}(t)$:

$$\frac{d^2 w_{m,n}(t)}{dt^2}+\lambda^2 w_{m,n}(t)=\frac{4P(t)}{ab\rho}\cdot\sin\frac{m\pi x(t)}{a}\cdot\sin\frac{n\pi y(t)}{b}, \quad (3)$$

where

$$\lambda^2=\frac{D}{\rho}\left[\left(\frac{m\pi}{a}\right)^2+\left(\frac{n\pi}{b}\right)^2\right]^2+\frac{N_a}{\rho}\left(\frac{m\pi}{a}\right)^2+\frac{N_b}{\rho}\left(\frac{n\pi}{b}\right)^2+\frac{k}{\rho}.$$

The solution of Eq. 3 depends upon the expressions $x(t)$, $y(t)$ and $P(t)$. The following particular applica-

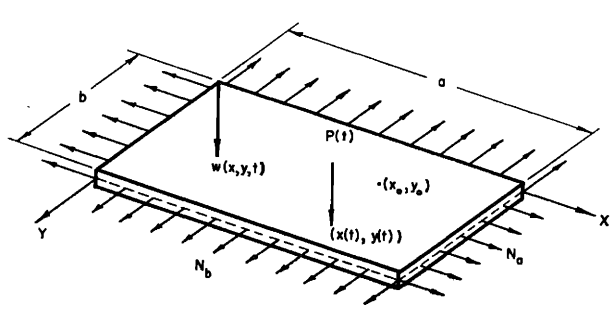

FIG. 1. Simply supported plate with a moving force.

[1] W. Nowacki, *Dynamics of Elastic Systems* (John Wiley & Sons, Inc., New York, 1963), Chap. 9, pp. 198–255.
[2] D. L. Holl, "Dynamic Loads on Thin Plates on Elastic Foundations" Proc. Symp. Appl. Math. **3**, 107–116 (1950).
[3] K. Piszczek, "Possibility of Dynamic Stability Loss Under Moving Concentrated Loads," Arch. Mech. Stos. **10**, 195–209 (1959).
[4] H. Reismann, "Dynamic Response of Elastic Plates to Moving Loads," Martin Co., Denver, Colo., Res. Rept. No. R-62-8, 1–89 (1962).
[5] R. Livesley, "Some Notes on the Mathematical Theory of a Loaded Elastic Plate Resting on an Elastic Foundation," Quart. J. Mech. Appl. Math. **6**, 32–44 (1953).
[6] L. S. D. Morley, "Elastic Plate with Loads Traveling at Uniform Velocity along the Bounding Surfaces," Quart. J. Mech. Appl. Math. **15**, 194–213 (1962).

tions are considered herein:

Case 1: Time dependent point force oscillating with amplitude X about the plate position (x_0, y_0) for which

$$P(t)=P\cos\omega t,$$
$$x(t)=x_0+X\sin\beta t,$$

and

$$y(t)=y_0. \tag{4}$$

Case 2: Point force of constant magnitude traveling in a circular orbit of radius R about the plate position (x_0, y_0) for which

$$P(t)=P,$$
$$x(t)=x_0+R\cos\beta t,$$

and

$$y(t)=y_0+R\sin\beta t. \tag{5}$$

A. Case 1—Oscillating Point Force

Substituting Eq. 4 into Eq. 2 yields

$$\frac{d^2w_{m,n}(t)}{dt^2}+\lambda^2 w_{m,n}(t)=\frac{4P}{ab\rho}\cos\omega t\cdot\sin\frac{n\pi y_0}{b}\cdot\sin\frac{m\pi}{a}(x_0+X\sin\beta t). \tag{6}$$

By introducting the dimensionless ratios

$$\tau=(\pi^2/a^2)(D/\rho)^{\frac{1}{2}}t, \qquad \alpha_4=ka^4/D\pi^4, \qquad \bar{\omega}=\frac{\omega}{(\pi^2/a^2)(D/\rho)^{\frac{1}{2}}},$$
$$\alpha_1=a/b, \qquad A_m=m\pi x_0/a, \qquad \bar{\beta}=\frac{\beta}{(\pi^2/a^2)(D/\rho)^{\frac{1}{2}}},$$
$$\alpha_2=(N_a/D)(a^2/\pi^2), \qquad A_n=n\pi y_0/b, \qquad L=4Pa^3/bD\pi^4,$$
$$\alpha_3=(N_b/D)(a^2/\pi^2), \qquad B_m=m\pi X/a, \qquad W(x,y,\tau)=(L/2)w(x,y,\tau), \tag{7}$$

Eq. 6 becomes

$$d^2w_{m,n}(\tau)/d\tau^2+\lambda^2 w_{m,n}(\tau)=L\cos\bar{\omega}\tau\sin A_n\sin(A_m+B_m\sin\bar{\beta}\tau), \tag{8}$$

where

$$\bar{\lambda}^2=[m^2+(\alpha_1 n)^2]^2+\alpha_2 m^2+\alpha_3(\alpha_1 n)^2+\alpha_4.$$

The solution of Eq. 8 is

$$w(m,n,\tau)=A_{mn}\sin\bar{\lambda}\tau+B_{mn}\cos\bar{\lambda}\tau+(L/\bar{\lambda})(I_1\sin\bar{\lambda}\tau-I_2\cos\bar{\lambda}\tau), \tag{9}$$

where A_{mn}, B_{mn} are arbitrary constants, and the integrals I_1, I_2 are:

$$I_1=\int\cos\bar{\omega}\tau\cos\bar{\lambda}\tau\sin(A_m+B_m\sin\bar{\beta}\tau)d\tau,$$

and

$$I_2=\int\cos\bar{\omega}\tau\sin\bar{\lambda}\tau\sin(A_m+B_m\sin\bar{\beta}\tau)d\tau. \tag{10}$$

The evaluation of Eq. 10 requires the use of the first two of the following Bessel function identities[7]:

$$\cos(B_m\sin\bar{\beta}\tau)=J_0(B_m)+2\sum_{i=1}^{\infty}J_{2i}(B_m)\cos 2i\bar{\beta}\tau,$$

$$\sin(B_m\sin\bar{\beta}\tau)=2\sum_{i=0}^{\infty}J_{2i+1}(B_m)\sin(2i+1)\bar{\beta}\tau,$$

$$\cos(B_m\cos\bar{\beta}\tau)=J_0(B_m)+2\sum_{i=1}^{\infty}(-1)^i J_{2i}(B_m)\cos 2i\bar{\beta}\tau,$$

[7] G. N. Watson, *A Treatise on the Theory of Bessel Functions* (Cambridge University Press, New York, 1952), p. 22.

and

$$\sin(B_m \cos\bar{\beta}\tau) = 2\sum_{i=0}^{\infty} (-1)^i J_{2i+1}(B_m) \cos(2i+1)\bar{\beta}\tau. \tag{11}$$

For convenience, let

$$\begin{aligned}
f_1&=\bar{\lambda}+\bar{\omega}, & f_6&=\bar{\lambda}-\bar{\omega}-2i\bar{\beta},\\
f_2&=\bar{\lambda}+\bar{\omega}, & f_7&=\bar{\lambda}+\bar{\omega}-(2i+1)\bar{\beta},\\
f_3&=\bar{\lambda}+\bar{\omega}+2i\bar{\beta}, & f_8&=\bar{\lambda}+\bar{\omega}+(2i+1)\bar{\beta},\\
f_4&=\bar{\lambda}+\bar{\omega}-2i\bar{\beta}, & f_9&=\bar{\lambda}-\bar{\omega}-(2i+1)\bar{\beta},\\
f_5&=\bar{\lambda}-\bar{\omega}+2i\bar{\beta}, & f_{10}&=\bar{\lambda}-\bar{\omega}+(2i+1)\bar{\beta}.
\end{aligned} \tag{12}$$

Then, I_1 and I_2 become:

$$\begin{aligned}
I_1=&\frac{\sin A_m}{2} J_0(B_m)\left(\frac{1}{f_1}\sin f_1\tau+\frac{1}{f_2}\sin f_2\tau\right)\\
&+\frac{\sin A_m}{2}\sum_{i=1}^{\infty} J_{2i}(B_m)\left(\frac{1}{f_3}\sin f_3\tau+\frac{1}{f_4}\sin f_4\tau+\frac{1}{f_5}\sin f_5\tau+\frac{1}{f_6}\sin f_6\tau\right)\\
&+\frac{\cos A_m}{2}\sum_{i=0}^{\infty} J_{2i+1}(B_m)\left(\frac{1}{f_7}\cos f_7\tau-\frac{1}{f_8}\cos f_8\tau-\frac{1}{f_9}\cos f_9\tau+\frac{1}{f_{10}}\cos f_{10}\tau\right),
\end{aligned} \tag{13}$$

and

$$\begin{aligned}
I_2=&-\frac{\sin A_m}{2} J_0(B_m)\left(\frac{1}{f_1}\cos f_1\tau+\frac{1}{f_2}\cos f_2\tau\right)\\
&-\frac{\sin A_m}{2}\sum_{i=1}^{\infty} J_{2i}(B_m)\left(\frac{1}{f_3}\cos f_3\tau+\frac{1}{f_4}\cos f_4\tau-\frac{1}{f_5}\cos f_5\tau+\frac{1}{f_6}\cos f_6\tau\right)\\
&+\frac{\cos A_m}{2}\sum_{i=0}^{\infty} J_{2i+1}(B_m)\left(\frac{1}{f_7}\sin f_7\tau-\frac{1}{f_8}\sin f_8\tau-\frac{1}{f_9}\sin f_9\tau+\frac{1}{f_{10}}\sin f_{10}\tau\right).
\end{aligned} \tag{14}$$

It can be shown that the formal interchange of summation and integration is justified, since infinite series of functions of the type

$$\sum_{i=0}^{\infty} J_i(z)\begin{cases}\cos it\\ \text{or}\\ \sin it\end{cases}$$

converge uniformly in t.

In the following analyses, two sets of initial conditions are considered which are designated herein as:

1. Drop load—Initially the plate is at rest and undeformed. At $\tau=0$ the load P is dropped from zero height at the plate position (x_0,y_0) and begins to oscillate longitudinally about x_0 and to change in magnitude according to $P\cos\bar{\omega}\tau$.

2. Static load—initially the plate is at rest with the static load P at (x_0,y_0). At $\tau=0$ the load begins to oscillate longitudinally about x_0 and to change in magnitude according to $P\cos\bar{\omega}\tau$.

Let

$$\begin{aligned}
S_mS_n&=\sin A_m \sin A_n \sin(m\pi x/a)\sin(n\pi y/b),\\
S_mC_n&=\sin A_m \cos A_n \sin(m\pi x/a)\sin(n\pi y/b),\\
C_mS_n&=\cos A_m \sin A_n \sin(m\pi x/a)\sin(n\pi y/b),
\end{aligned}$$

and

$$C_mC_n=\cos A_m \cos A_n \sin(m\pi x/a)\sin(n\pi y/b). \tag{15}$$

Substituting Eqs. 13 and 14 into Eq. 9, and recalling Eq. 2, the general solutions for the drop load $W_D(x,y,\tau)$ and static load $W_S(x,y,\tau)$, respectively, are given by:

Drop load:

$$W_D(x,y,\tau)=\sum_{m=1}^{\infty}\sum_{n=1}^{\infty}J_0(B_m)\left\{\frac{\cos\bar{\lambda}\tau}{\bar{\lambda}}\left(\frac{1}{f_1}\cos f_1\tau+\frac{1}{f_2}\cos f_2\tau-\frac{1}{f_1f_2}2\right)+\frac{\sin\bar{\lambda}\tau}{\bar{\lambda}}\left(\frac{1}{f_1}\sin f_1\tau+\frac{1}{f_2}\sin f_2\tau\right)\right\}S_mS_n$$

$$+\sum_{m=1}^{\infty}\sum_{n=1}^{\infty}\sum_{i=1}^{\infty}J_{2i}(B_m)\left\{\frac{\cos\bar{\lambda}\tau}{\lambda}\left(\frac{1}{f_3}\cos f_3\tau+\frac{1}{f_4}\cos f_4\tau+\frac{1}{f_5}\cos f_5\tau+\frac{1}{f_6}\cos f_6\tau-\frac{1}{f_3f_4}2f_1-\frac{1}{f_5f_6}2f_2\right)\right.$$

$$\left.+\frac{\sin\bar{\lambda}\tau}{\bar{\lambda}}\left(\frac{1}{f_3}\sin f_3\tau+\frac{1}{f_4}\sin f_4\tau+\frac{1}{f_5}\sin f_5\tau+\frac{1}{f_6}\sin f_6\tau\right)\right\}S_mS_n$$

$$+\sum_{m=1}^{\infty}\sum_{n=1}^{\infty}\sum_{i=0}^{\infty}J_{2i+1}(B_m)\left\{\frac{\cos\bar{\lambda}\tau}{\bar{\lambda}}\left(\frac{1}{f_8}\sin f_8\tau-\frac{1}{f_7}\sin f_7\tau+\frac{1}{f_{10}}\sin f_{10}\tau-\frac{1}{f_9}\sin f_9\tau\right)\right.$$

$$\left.+\frac{\sin\bar{\lambda}\tau}{\bar{\lambda}}\left[\frac{1}{f_7}\cos f_7\tau-\frac{1}{f_8}\cos f_8\tau-\frac{1}{f_{10}}\cos f_{10}\tau+\frac{1}{f_9}\cos f_9\tau-2(2i+1)\bar{\beta}\left(\frac{1}{f_7f_8}+\frac{1}{f_9f_{10}}\right)\right]\right\}C_mS_n. \quad (16)$$

Static load:

$$W_S(x,y,\tau)=W_D(x,y,\tau)+2\sum_{m=1}^{\infty}\sum_{n=1}^{\infty}\frac{\cos\bar{\lambda}\tau}{\lambda^2}S_mS_n. \quad (17)$$

Equations 16 and 17 give the dimensionless deflection for any plate position (x,y) at time τ for the load $P\cos\bar{\omega}\tau$ oscillating with amplitude X about the plate position (x_0,y_0). In particular, the deflection under the load is obtained by setting $x=x_0+\sin\bar{\beta}\tau$ and $y=y_0$. Resonance occurs whenever any of the following relationships is satisfied:

$$\begin{aligned}\bar{\lambda}&=\bar{\omega},\\ \bar{\lambda}+\bar{\omega}&=2i\bar{\beta},\\ |\bar{\lambda}-\bar{\omega}|&=2i\bar{\beta},\\ \bar{\lambda}+\bar{\omega}&=(2i+1)\bar{\beta},\end{aligned} \quad (18)$$

and

$$|\bar{\lambda}-\bar{\omega}|=(2i+1)\bar{\beta}.$$

It should be noted that if one of the above resonance conditions is satisfied, the corresponding expressions in Eqs. 16 and 17 are indeterminate and must be modified by a suitable limiting procedure. For example, if $\bar{\lambda}=\bar{\omega}$, the terms containing the zero-order Bessel function are indeterminate; in the limit, these terms become

$$\lim_{\bar{\lambda}\to\bar{\omega}}\sum_{m=1}^{\infty}\sum_{n=1}^{\infty}J_0(B_m)\frac{\cos\bar{\lambda}\tau}{\bar{\lambda}}\left(\frac{1}{f_1}\cos f_1\tau+\frac{1}{f_2}\cos f_2\tau-\frac{1}{f_1f_2}2\bar{\lambda}\right)S_mS_n=J_0(B_m)[(\cos\bar{\lambda}\tau)/\bar{\lambda}]\frac{1}{2\bar{\omega}}[\cos(2\bar{\omega}\tau)-1]S_mS_n$$

and

$$\lim_{\bar{\lambda}\to\bar{\omega}}\sum_{m=1}^{\infty}\sum_{n=1}^{\infty}J_0(B_m)\frac{\sin\bar{\lambda}\tau}{\bar{\lambda}}\left(\frac{1}{f_1}\sin f_1\tau+\frac{1}{f_2}\sin f_2\tau\right)S_mS_n=J_0(B_m)\frac{\sin\bar{\lambda}\tau}{\bar{\lambda}}\left(\frac{1}{2\bar{\omega}}\sin 2\bar{\omega}\tau+\tau\right)S_mS_n.$$

These equations show that the amplitude of plate vibration increases linearly with time. Similarly, if resonance occurs for any of the remaining relationships, the corresponding amplitude terms can also be shown to increase linearly with time.

B. Case 2—Circularly Orbiting Point Force

Substituting Eq. 5 into Eq. 4 gives

$$\frac{d^2w}{d\tau^2}_{m,n}(t)+\lambda^2w_{m,n}(t)=\frac{1}{ab\rho}4P\sin\frac{m\pi}{a}(x_0+R\cos\beta t)\sin\frac{n\pi}{b}(y_0+R\sin\beta t). \quad (19)$$

Introducing the previously defined dimensionless ratios and, in addition, setting $R_m=m\pi R/a$ and $R_n=n\pi R/b$, Eq. 19 becomes

$$(d^2w/(d\tau^2)_{m,n}(\tau)+\bar{\lambda}^2w_{m,n}(\tau)=L\sin(A_m+R_m\cos\bar{\beta}\tau)\sin(A_n+R_n\sin\bar{\beta}\tau). \tag{20}$$

The solution of Eq. 20 is

$$w_{m,n}(\tau)=A_{mn}\sin\bar{\lambda}\tau+B_{mn}\cos\bar{\lambda}\tau+w_{m,n}(\tau)_p, \tag{21}$$

where $w_{m,n}(\tau)_p$ is the particular solution. Let

$$\begin{aligned}
g_1&=\bar{\lambda}+2j\bar{\beta}, & g_{11}&=\bar{\lambda}+2(i+j)\bar{\beta},\\
g_2&=\bar{\lambda}-2j\bar{\beta}, & g_{12}&=\bar{\lambda}-2(i+j)\bar{\beta},\\
g_3&=\bar{\lambda}+2i\bar{\beta}, & g_{13}&=\bar{\lambda}+2(i-j)\bar{\beta},\\
g_4&=\bar{\lambda}-2i\bar{\beta}, & g_{14}&=\bar{\lambda}-2(i-j)\bar{\beta},\\
g_5&=\bar{\lambda}-(2j+1)\bar{\beta}, & g_{15}&=\bar{\lambda}+(2i+1)\bar{\beta},\\
g_6&=\bar{\lambda}+(2j+1)\bar{\beta}, & g_{16}&=\bar{\lambda}-(2i+1)\bar{\beta},\\
g_7&=\bar{\lambda}-(2i+2j+1)\bar{\beta}, & g_{17}&=\bar{\lambda}+(2i-2j+1)\bar{\beta},\\
g_8&=\bar{\lambda}+(2i+2j+1)\bar{\beta}, & g_{18}&=\bar{\lambda}-(2i-2j+1)\bar{\beta},\\
g_9&=\bar{\lambda}+(2i-2j+1)\bar{\beta}, & g_{19}&=\bar{\lambda}-2(i+j+1)\bar{\beta},\\
g_{10}&=\bar{\lambda}-(2i-2j-1)\bar{\beta}, & g_{20}&=\bar{\lambda}+2(i+j+1)\bar{\beta}.
\end{aligned} \tag{22}$$

Proceeding as in *Case 1*, the general solutions for the drop load and static load, respectively, are given by:

Drop load:

$$\begin{aligned}
W_D(x,y,\tau)=\sum_{m=1}^{\infty}\sum_{n=1}^{\infty}\Bigg\{&J_0(R_m)J_0(R_n)\frac{1}{\bar{\lambda}^2}(1-\cos\bar{\lambda}\tau)+\sum_{j=1}^{\infty}J_0(R_m)J_{2j}(R_n)\frac{\sin\bar{\lambda}\tau}{\bar{\lambda}}\\
&+\sum_{j=1}^{\infty}J_0(R_m)J_{2j}(R_n)\frac{\sin\bar{\lambda}\tau}{\bar{\lambda}}\left(\frac{1}{g_1}\sin g_1\tau+\frac{1}{g_2}\sin g_2\tau\right)\\
&+\sum_{j=1}^{\infty}J_0(R_m)J_{2j}(R_n)\frac{\cos\bar{\lambda}\tau}{\bar{\lambda}}\left(\frac{1}{g_1}\cos g_1\tau+\frac{1}{g_2}\cos g_2\tau\right)\\
&+\sum_{i=1}^{\infty}(-1)^iJ_0(R_n)J_{2i}(R_m)\frac{\sin\bar{\lambda}\tau}{\bar{\lambda}}\left(\frac{1}{g_3}\sin g_3\tau+\frac{1}{g_4}\sin g_4\tau\right)\\
&+\sum_{i=1}^{\infty}(-1)^iJ_0(R_n)J_{2i}(R_m)\frac{\cos\bar{\lambda}\tau}{\bar{\lambda}}\left(\frac{1}{g_3}\cos g_3\tau+\frac{1}{g_4}\cos g_4\tau\right)\Bigg\}S_mS_n\\
&+\sum_{m=1}^{\infty}\sum_{n=1}^{\infty}\sum_{j=0}^{\infty}J_0(R_m)J_{j+1}(R_n)\Bigg\{\frac{\sin\bar{\lambda}\tau}{\bar{\lambda}}\left(\frac{1}{g_5}\cos g_5\tau-\frac{1}{g_6}\cos g_6\tau\right.\\
&\left.-\frac{1}{g_5g_6}2(2j+1)\bar{\beta}\right)+\frac{\cos\bar{\lambda}\tau}{\bar{\lambda}}\left(\frac{1}{g_6}\sin g_6\tau-\frac{1}{g_5}\sin g_5\tau\right)\Bigg\}S_mC_n\\
&+\sum_{m=1}^{\infty}\sum_{n=1}^{\infty}\sum_{i=0}^{\infty}(-1)^iJ_0(R_n)J_{2i+1}(R_m)\Bigg\{\frac{\sin\bar{\lambda}\tau}{\bar{\lambda}}\left(\frac{1}{g_{15}}\sin g_{15}\tau+\frac{1}{g_{16}}\sin g_{16}\tau\right)\\
&+\frac{\cos\bar{\lambda}\tau}{\bar{\lambda}}\left(\frac{1}{g_{15}}\cos g_{15}\tau+\frac{1}{g_{16}}\cos g_{16}\tau-\frac{1}{g_{15}g_{16}}2\bar{\lambda}\right)\Bigg\}S_nC_m
\end{aligned}$$

$$+\sum_{m=1}^{\infty}\sum_{n=1}^{\infty}\sum_{i=1}^{\infty}\sum_{j=0}^{\infty}(-1)^{i}J_{2i}(R_m)J_{2j+1}(R_n)\left\{\frac{\sin\bar{\lambda}\tau}{\bar{\lambda}}\left(\frac{1}{g_7}\cos g_7\tau-\frac{1}{g_8}\cos g_8\tau+\frac{1}{g_9}\cos g_9\tau\right.\right.$$

$$\left.-\frac{1}{g_{10}}\cos g_{10}\tau-\frac{1}{g_7g_8}2(2i+2j+1)\bar{\beta}+\frac{1}{g_9g_{10}}2(2i-2j-1)\bar{\beta}\right)$$

$$\left.+\frac{\cos\bar{\lambda}\tau}{\bar{\lambda}}\left(\frac{1}{g_8}\sin g_8\tau-\frac{1}{g_7}\sin g_7\tau+\frac{1}{g_{10}}\sin g_{10}\tau-\frac{1}{g_9}\sin g_9\tau\right)\right\}S_mC_n$$

$$+\sum_{m=1}^{\infty}\sum_{n=1}^{\infty}\sum_{i=0}^{\infty}\sum_{j=1}^{\infty}(-1)^{i}J_{2j}(R_n)J_{2i+1}(R_m)\left\{\frac{\cos\bar{\lambda}\tau}{\bar{\lambda}}\left(\frac{1}{g_8}\cos g_8\tau\right.\right.$$

$$+\frac{1}{g_7}\cos g_7\tau+\frac{1}{g_{17}}\cos g_{17}\tau+\frac{1}{g_{18}}\cos g_{18}\tau-2\bar{\lambda}\left(\frac{1}{g_7g_8}+\frac{1}{g_{17}g_{18}}\right)\Big)$$

$$\left.+\frac{\sin\bar{\lambda}\tau}{\bar{\lambda}}\left(\frac{1}{g_8}\sin g_8\tau+\frac{1}{g_7}\sin g_7\tau+\frac{1}{g_{17}}\sin g_{17}\tau+\frac{1}{g_{18}}\sin g_{18}\tau\right)\right\}S_nC_m$$

$$+\sum_{m=1}^{\infty}\sum_{n=1}^{\infty}\sum_{i=1}^{\infty}\sum_{j=1}^{\infty}(-1)^{i}J_{2i}(R_m)J_{2j}(R_n)\left\{\frac{\sin\bar{\lambda}\tau}{\bar{\lambda}}\left(\frac{1}{g_{11}}\sin g_{11}\tau\right.\right.$$

$$+\frac{1}{g_{12}}\sin g_{12}\tau+\frac{1}{g_{13}}\sin g_{13}\tau+\frac{1}{g_{14}}\sin g_{14}\tau\Big)+\frac{\cos\bar{\lambda}\tau}{\bar{\lambda}}\left(\frac{1}{g_{11}}\cos g_{11}\tau+\frac{1}{g_{12}}\sin g_{12}\tau\right.$$

$$\left.\left.+\frac{1}{g_{13}}\cos g_{13}\tau+\frac{1}{g_{14}}\sin g_{14}\tau+2\bar{\lambda}\left(\frac{1}{g_{11}g_{12}}+\frac{1}{g_{13}g_{14}}\right)\right)\right\}S_mS_n$$

$$+\sum_{m=1}^{\infty}\sum_{n=1}^{\infty}\sum_{i=0}^{\infty}\sum_{j=0}^{\infty}(-1)^{i}J_{2i+1}(R_n)J_{2j+1}(R_m)\left\{\frac{\sin\bar{\lambda}\tau}{\bar{\lambda}}\left(\frac{1}{g_{19}}\cos g_{19}\tau\right.\right.$$

$$\left.-\frac{1}{g_{20}}\cos g_{20}\tau+\frac{1}{g_{13}}\cos g_{13}\tau-\frac{1}{g_{14}}\cos g_{14}\tau-\frac{1}{g_{19}g_{20}}4(i+j+1)\bar{\beta}+\frac{1}{g_{13}g_{14}}4(i-j)\bar{\beta}\right)$$

$$\left.+\frac{\cos\bar{\lambda}\tau}{\bar{\lambda}}\left(\frac{1}{g_{20}}\sin g_{20}\tau-\frac{1}{g_{19}}\sin g_{19}\tau+\frac{1}{g_{14}}\sin g_{14}\tau-\frac{1}{g_{13}}\sin g_{13}\tau\right)\right\}C_mC_n. \quad (23)$$

Static load:

$$W_S(x,y,\tau)=W_D(x,y,\tau)+4\sum_{m=1}^{\infty}\sum_{n=1}^{\infty}\frac{\cos\bar{\lambda}\tau}{\bar{\lambda}^2}(\sin A_m\sin A_n\cos B_m+\cos A_m\sin A_n\sin B_m)\sin\frac{m\pi x}{a}\sin\frac{n\pi y}{b}. \quad (24)$$

Equations 23 and 24 give the dimensionless deflection for any plate position (x,y) at time τ for the load P traversing a circular orbit of radius R about the plate position (x_0,y_0). In particular, the deflection under the load is obtained by setting $x=x_0+R\cos\bar{\beta}\tau$ and $y=y_0+R\sin\bar{\beta}\tau$. Resonance occurs whenever any of the relationships given by Eq. 25 is satisfied.

$$\begin{aligned}
&\bar{\lambda}=2i\bar{\beta}, && \bar{\lambda}=2i-j\bar{\beta},\\
&\bar{\lambda}=2j\bar{\beta}, && \bar{\lambda}=(2i+2j+1)\bar{\beta},\\
&\bar{\lambda}=(2i+1)\bar{\beta}, && \bar{\lambda}=|2i-2j+1|\bar{\beta}, \quad (25)\\
&\bar{\lambda}=(2j+1)\bar{\beta}, && \bar{\lambda}=|2i-2j-1|\bar{\beta},\\
&\bar{\lambda}=2(i+j)\bar{\beta}, && \bar{\lambda}=2(i+j+1)\bar{\beta}.
\end{aligned}$$

It should be noted again that if one of these resonance conditions is satisfied, the corresponding expression in Eq. 23 and 24 must be modified as outlined in *Case 1*, above. The corresponding plate amplitude increases linearly with time.

The convergence of the quadruple infinite series given above proved to be very rapid for the illustrations presented herein. However, it is entirely possible, for certain select set of parameters, that the convergence may prove to be rather slow.

II. DISCUSSION AND NUMERICAL RESULTS

If X, R, and $\bar{\omega}$ are set equal to zero, Eqs. 16, 17 and Eqs. 23, 24 reduce to the well-known solutions for a

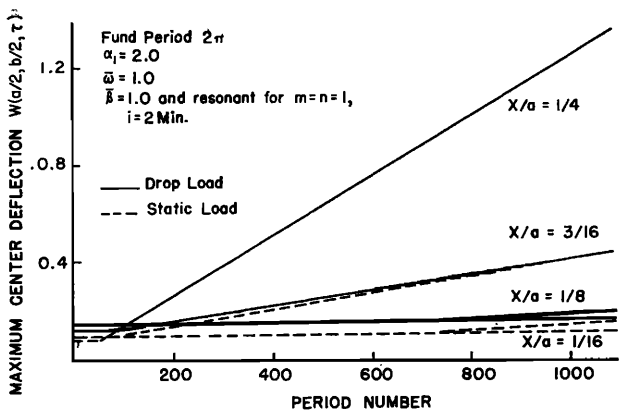

FIG. 2. Rectangular plate deflection buildup for oscillating point force at nonresonant frequency $\bar{\omega}$ and resonant frequency $\bar{\beta}$.

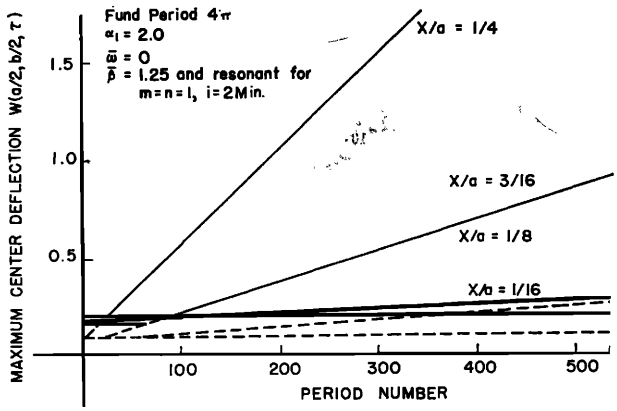

FIG. 3. Rectangular plate deflection buildup for oscillating point force at resonant frequency $\bar{\beta}$.

point force concentrated at (x_0, y_0) with initial conditions corresponding to either the drop load or static load case, respectively.

The deflection at the center of the plate due to the above loads accelerating about the center of the plate may be determined by introducing the following simplifying relationships:

$$\begin{aligned}
&\sin A_m \sin A_n \sin(m\pi x/a) \sin(n\pi y/b) = \\
&\qquad 1 \text{ for } m, n = 1, 3, 5\cdots \\
&\qquad 0 \text{ for } m, n = 2, 4, 6\cdots, \\
&\sin A_m \cos A_n \sin(m\pi x/a) \sin(n\pi y/b) = 0, \\
&\cos A_m \sin A_n \sin(m\pi x/a) \sin(n\pi y/b) = 0, \\
&\cos A_m \cos A_n \sin(m\pi x/a) \sin(n\pi y/b) = 0, \\
&\text{for } x = x_0 = a/2 \text{ and } y = y_0 = b/2.
\end{aligned} \tag{26}$$

For this special case the resonance conditions reduce to:

(1) Oscillating force—

$$\begin{aligned}
\bar{\lambda} &= \bar{\omega}, \\
\bar{\lambda} + \bar{\omega} &= 2i\bar{\beta}, \\
|\bar{\lambda} - \bar{\omega}| &= 2i\bar{\beta}.
\end{aligned} \tag{27}$$

(2) Circularly orbiting force—

$$\begin{aligned}
\bar{\lambda} &= 2i\beta, \\
\bar{\lambda} &= 2j\bar{\beta}, \\
\bar{\lambda} &= 2(i+j)\bar{\beta}, \\
\bar{\lambda} &= 2|i-j|\bar{\beta}.
\end{aligned} \tag{28}$$

Because the general deflection equations are exceedingly cumbersome, it is difficult to interpret their characteristic behavior. To illustrate the dynamic response of the plate most effectively, it is convenient to consider the load as accelerating about the center of the plate, and to determine the deflection at this point.

Preliminary calculations show that the lower-order terms in the deflection equations are predominant. Thus, the characteristic behavior of the plate may best be illustrated by simple examples restricted to the fundamental mode of vibration ($m=m=1$). Numerical results for the deflection at the center of a rectangular plate are presented for both the oscillating and circularly orbiting point forces. Comparisons are made for the deflection profiles and rate of buildup of center deflection for $\alpha_2=\alpha_3=\alpha_4=0$ and $\alpha_1=2$, where the α's are given by Eq. 7.

Figures 2–9 represent typical deflection profiles and rate of deflection buildup curves for X/a or R/a amplitude ratios of $\frac{1}{16}$, $\frac{1}{8}$, $\frac{3}{16}$, and $\frac{1}{4}$. The nonresonant deflection profiles shown are the deflection-time histories at the center of the plate throughout a fundamental plate period. The fundamental plate period is defined as the time interval for which the deflection profile repeats itself. The deflection buildup curves represent the approximate envelope of maximum deflections that occur

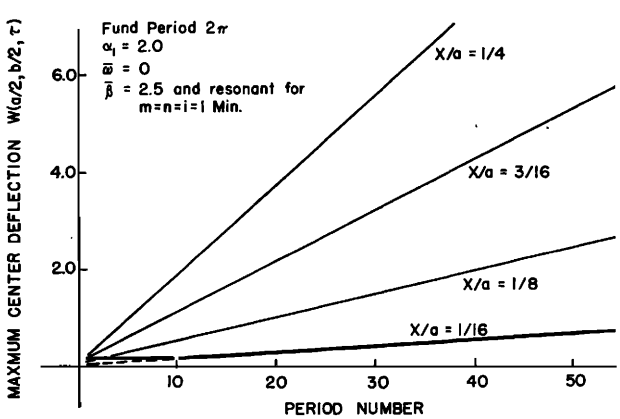

FIG. 4. Rectangular plate deflection buildup for oscillating point force at resonant frequency $\bar{\beta}$.

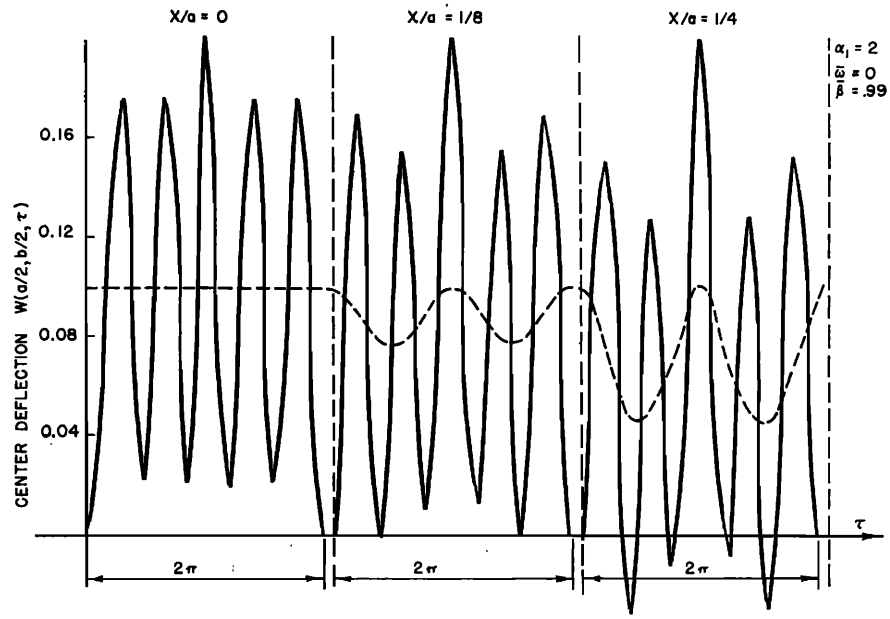

FIG. 5. Rectangular plate deflection profiles for oscillating point force at nonresonant frequency $\bar{\beta}$.

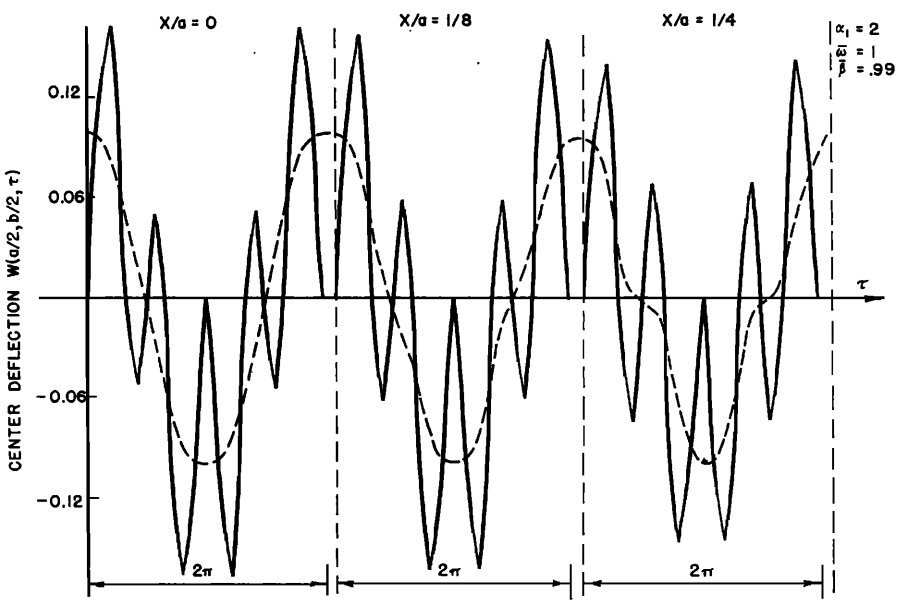

FIG. 6. Rectangular plate deflection profiles for oscillating point force at nonresonant frequencies $\bar{\omega}$ and $\bar{\beta}$.

during each fundamental plate period for the amplitude ratios given above.

Figures 2–6 present the results of an oscillating point force operating at either a resonant frequency $\bar{\beta}$ or nonresonant frequencies $\bar{\omega}$ and $\bar{\beta}$. Figures 2 and 3 show that the rate of deflection buildup is greatest for $\bar{\omega}$ equal to zero. Figures 3 and 4 show that the rate of deflection buildup is considerably greater at a frequency $\bar{\beta}$ that causes resonance of the plate for a Bessel function of order two ($i=1$) than for a Bessel function of order four ($i=2$). Figure 5 shows that the maximum deflection at the center of the plate does not change appreciably with increasing amplitude ratio X/a for $\bar{\omega}$ equal to zero, while Fig. 6 shows the added influence of the nonresonant frequency $\bar{\omega}$.

Figures 7–9 present the results of a circularly orbiting point force operating at both a resonant and nonresonant frequency $\bar{\beta}$. Figure 7 shows that the maximum deflection of the plate decreases with an increasing R/a amplitude ratio. Figures 8 and 9 show that the rate of deflection buildup is greatest at a frequency $\bar{\beta}$ which causes resonance of the plate for Bessel functions of order two ($i=j=1$) than for Bessel functions of order four ($i=j=2$).

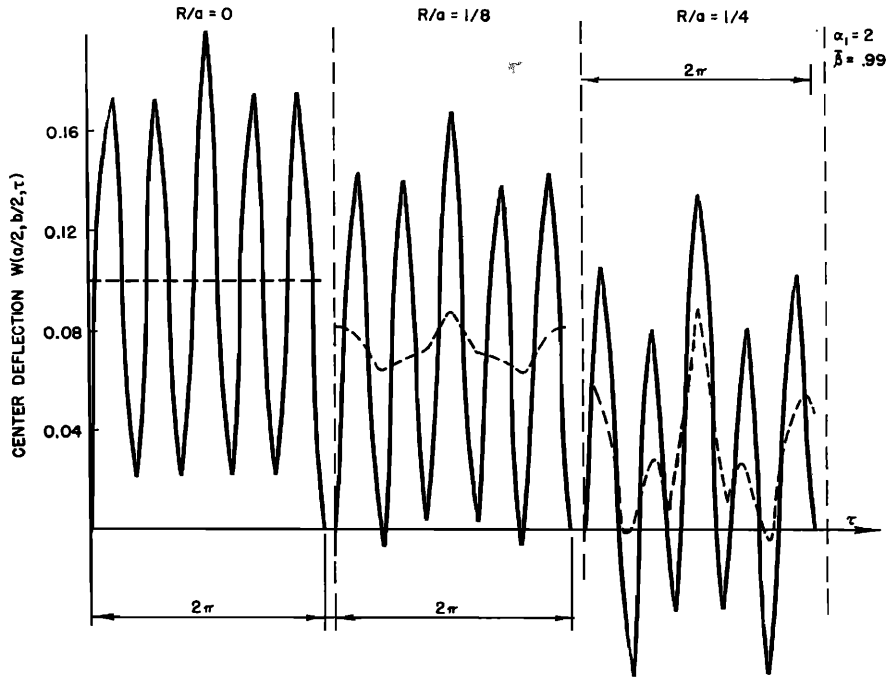

FIG. 7. Rectangular plate deflection profiles for circularly orbiting point force at nonresonant frequency $\bar{\beta}$.

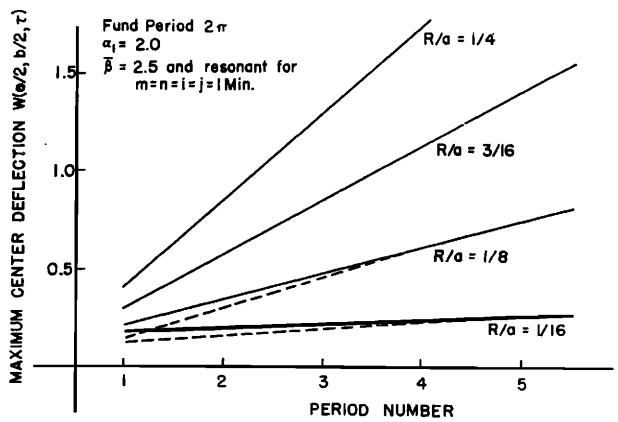

FIG. 8. Rectangular plate deflection buildup for circularly orbiting point force at resonant frequency $\bar{\beta}$.

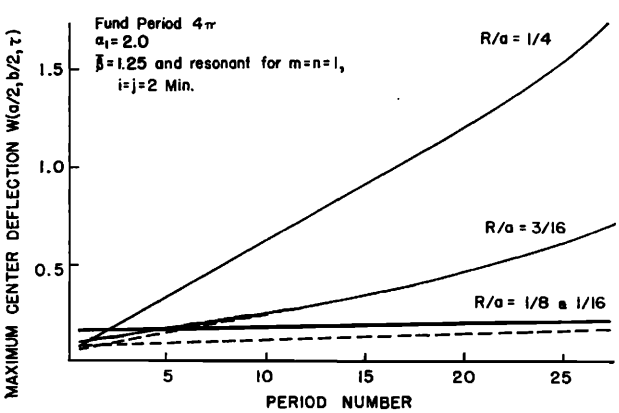

FIG. 9. Rectangular plate deflection buildup for circularly orbiting point force at resonant frequency β.

For the curves presented herein, an increase in the amplitude ratio X/a or R/a is accompanied by a corresponding increase in the rate of deflection buildup. But, for a system resonating at higher modes of vibration, it is possible to have an increase in both of these amplitude ratios and yet obtain a decrease in the rate of deflection buildup. This results since the rate of deflection buildup is primarily dependent upon the order and argument of the Bessel function. For example, the values of a Bessel function of order two ($i=1$) for X/a

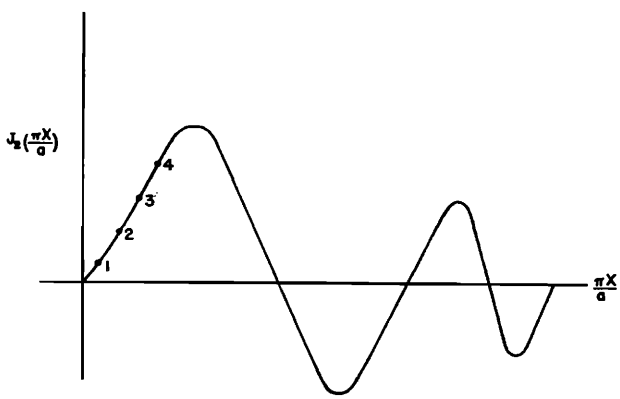

FIG. 10. Bessel function of order two for $m=1$.

For point 1, $X/a=\frac{1}{16}$, $J_2=0.00479$

2, $X/a=\frac{1}{8}$, $J_2=0.01896$

3, $X/a=\frac{3}{16}$, $J_2=0.04199$

4, $X/a=\frac{1}{4}$, $J_2=0.07297$

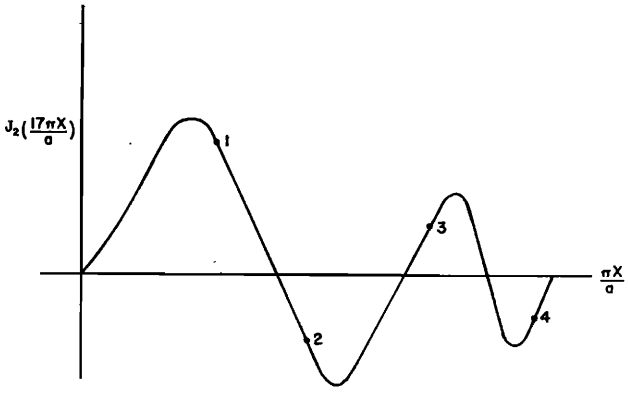

FIG. 11. Bessel function of order two for $m=17$.

For point 1, $X/a=\frac{1}{16}$, $J_2=0.47568$
2, $X/a=\frac{1}{8}$, $J_2=-0.31328$
3, $X/a=\frac{3}{16}$, $J_2=0.25466$
4, $X/a=\frac{1}{4}$, $J_2=-0.21822$

ratios of $\frac{1}{16}$ to $\frac{1}{4}$ are given in ascending order in Fig. 10 for the plate vibrating at a mode given by $m=1$ and n arbitrary. Figure 11 presents the values of a Bessel function of order two ($i=1$) for X/a ratios of $\frac{1}{16}$ to $\frac{1}{4}$ in the order shown for the plate vibrating at a mode given by $m=17$ and n arbitrary.

III. CONCLUSIONS

For a variable magnitude force $P\cos\bar{\omega}\tau$, whose instantaneous position on the plate is given by $(x_0+X\times\sin\bar{\beta}\tau, y_0)$, resonance occurs whenever any one of the following conditions is satisfied:

$$C_1. \quad \bar{\lambda}=\bar{\omega}$$

$$\left.\begin{array}{ll} C_2. & \bar{\lambda}+\bar{\omega}=2i\bar{\beta} \\ C_3. & |\bar{\lambda}-\bar{\omega}|=2i\bar{\beta} \end{array}\right\} i=i,\ 2,\cdots\infty,$$

$$\left.\begin{array}{ll} C_4. & \bar{\lambda}+\bar{\omega}=(2i+1)\bar{\beta} \\ C_5. & |\bar{\lambda}-\bar{\omega}|=(2i+1)\bar{\beta} \end{array}\right\} i=0,\ 1,\cdots\infty.$$

Condition 1 corresponds to the ordinary resonance produced by a variable magnitude force $P\cos\bar{\omega}\tau$ concentrated at a fixed plate position. Conditions 2–5 predict a resonance which is due to the longitudinal oscillation of the force along the plate. For a constant-magnitude force P whose instantaneous position on the plate is given by $(x_0+R\cos\bar{\beta}\tau,\ y_0+R\sin\bar{\beta}\tau)$, resonance occurs for any of the relationships given by Eq. 25 and is due to the changing position of the point force on the plate. For both types of loading, the rate of deflection buildup depends primarily on the Bessel function for each mode of vibration.